Functional Proteomics Study Reveals That *N*-Acetylglucosaminyltransferase V Reinforces the Invasive/Metastatic Potential of Colon Cancer through Aberrant Glycosylation on Tissue Inhibitor of Metalloproteinase-1*[S]

Yong-Sam Kim‡, Soo Young Hwang‡, Hye-Yeon Kang‡, Hosung Sohn‡, Sejeong Oh§, Jin-Young Kim¶, Jong Shin Yoo¶, Young Hwan Kim¶, Cheorl-Ho Kim‖, Jae-Heung Jeon, Jung Mi Lee‡‡, Hyun Ah Kang‡‡, Eiji Miyoshi§§, Naoyuki Taniguchi§§, Hyang-Sook Yoo‡, and Jeong-Heon Ko‡¶¶**

N-Acetylglucosaminyltransferase-V (GnT-V) has been reported to be up-regulated in invasive/metastatic cancer cells, but a comprehensive understanding of how the transferase correlates with the invasive/metastatic potential is not currently available. Through a glycomics approach, we identified 30 proteins, including tissue inhibitor of metalloproteinase-1 (TIMP-1), as a target protein for GnT-V in human colon cancer cell WiDr. TIMP-1 was aberrantly glycosylated as characterized by the addition of β1,6-*N*-acetylglucosamine, polylactosaminylation, and sialylation in GnT-V-overexpressing WiDr cells. Compared with normal TIMP-1, the aberrantly glycosylated TIMP-1 showed the weaker inhibition on both matrix metalloproteinase (MMP)-2 and MMP-9, and this aberrancy was closely associated with cancer cell invasion and metastasis *in vivo* as well as *in vitro*. Integrated data, both of TIMP-1 expression level and aberrant glycosylation, could provide important information to aid to improve the clinical outcome of colon cancer patients.   *Molecular & Cellular Proteomics 7:1–14, 2008.*

Cancer is a very complicated process, characterized by the uncontrolled, unbalanced overgrowth of malignant cells. The complexity of oncogenic processes and cancer progressions has demanded the discovery of biomarkers with a high sensitivity and specificity for diagnosis, prognosis, diseases monitoring, and therapeutic response prediction. Unfortunately, a discrete biomarker for colon cancer has yet to be discovered, although nearly 800,000 new colorectal cancer cases are thought to globally occur each year, which account for ~10% of all incident cancers, and the mortality from colorectal cancer is estimated at nearly 450,000 per year (1). *MLI1* and *MSH* genes are associated with hereditary non-polyposis colon cancer (2), and the *APC* gene is associated with familial adenomatous polyposis (3), but those factors fail to account for an occurrence of wide range of colon cancer. Moreover, colon cancer is one of the epithelium-derived cancers in which the circumstantial factors govern over hereditary genetic factors. These require a clear marker that serves as tracer molecule for the efficacious treatment of colon cancer.

Recent proteomics have focused on a dynamic alteration of post-translational modification of proteins, and many lines of evidence indicate that changes in post-translational modification of proteins are closely associated with the pathogenic processes of cells. An aberrant glycosylation induced by *N*-acetylglucosaminyltransferase V (GnT-V),[1] is a representative example of such protein modification as is implicated in tumor progression. An increase in β1,6-branching on *N*-linked glycans is associated with metastatic potential of cancer cells (4). Several target molecules for GnT-V were proposed to be involved in cancer progressions, including matriptase (5), β_1 integrin (6), and N-cadherin (7). However, those proteins are membrane-bound proteins and were not demonstrated to be aberrantly glycosylated in sera or tissues of cancer patients. Recent work stresses the discrete roles of the microenviron-

[1] The abbreviations used are: GnT-V, *N*-acetylglucosaminyltransferase V; DSA, *Datura stramonium* agglutinin; Gal, galactose; GlcNAc, *N*-acetylglucosamine; L-PHA, phytohemagglutinin-L$_4$; MMP, metalloproteinase; Neu, *N*-acetylneuraminic acid; TIMP, tissue inhibitor of metalloproteinase; rTIMP-1, TIMP-1 recombinant protein.

ment of tumor cells, referred to as "stroma," and documents its importance in supporting tumor progression (8). Cancer cells modulate their stromal environments by secreting various molecules, including growth factors, proteases, and extracellular matrix molecules (9–11). Many of the secreted proteins are glycoproteins, which prompted us to identify secreted glycoproteins that undergo aberrant glycosylation and are functionally responsible for cancer progression. For this, we adopted proteomics and glycomics techniques in which two-dimensional electrophoresis, lectin blot analysis, and MS-based protein identification were linked. We have previously reported that these approaches allowed us to identify several candidate proteins that are assumed to be involved in progressions of gastric cancer (12) and colon cancer (13) and have validated these approaches for discovery of biomarker by showing the role of aberrant glycosylation of protein tyrosine phosphatase κ as an example in cancer cell migration (13). In this article, we report that additional candidate proteins were identified including tissue inhibitor of metalloproteinase-1 (TIMP-1) as the target for GnT-V and, more importantly, that the aberrant glycosylation of TIMP-1 is closely correlated with invasive/metastatic potential of colon cancer cell WiDr.

EXPERIMENTAL PROCEDURES

Establishment of GnT-V and TIMP-1 Transfectants—Recombinant vectors *MGAT5*/pCXN (neo) were transfected into WiDr, a derivative of the human colonic adenocarcinoma cell line HT-29 (14), using Lipofectamine Plus Reagent (Invitrogen) according to the manufacturer's instructions, and the stable transfectants (WiDr:GnT-V) and the control cells (WiDr:mock) were established. TIMP-1 mutant genes were generated using the standard Megaprimer methods, where either or both Asn[30] and Asn[78] were changed to Gln. Wild-type *TIMP-1* and the mutant genes were cloned into pcDNA 3.1 hygro(+) plasmid vector (Invitrogen). The cloned vectors were transfected into WiDr: mock or WiDr:GnT-V cells. The stable TIMP-1 transfectants were confirmed by immunoblot analysis. Cells were maintained as monolayer in RPMI 1640 medium containing 10% fetal bovine serum at 37 °C, supplied with 5% CO_2.

Two-dimensional Electrophoresis and Mass Spectrometry—WiDr cells were cultured in a serum-free RPMI 1640 media for 3 days. From the media protein samples were prepared and subjected to two-dimensional electrophoretic analysis as described previously (12). For comparison of the expression level, 50 μg of proteins was minimally labeled with cy3- or cy5-fluorescent dyes following two-dimensional differential in-gel electrophoresis, according to the manufacturer's instructions. Fluorescence was measured with a Typoon 9410 Imager system (GE Healthcare), and an image analysis was performed using a Phoretix software (PerkinElmer Life Sciences). The protein spots of interest were excised, destained, and tryptic-digested using modified porcine trypsin (Promega). If necessary, the recovered peptides were desalted, concentrated using C18 ZipTips (Millihore), eluted with 50% (v/v) acetonitrile:water, and lyophilized. The lyophilized peptide samples were dissolved in 0.1% formic acid for LC-MS/MS. All MS/MS experiments for peptide identification were performed using a nano-LC/MS system consisting of an ultimate HPLC system and a Q-TOF mass spectrometer (Waters) equipped with a nano-ESI source. Ten microliters of each sample was loaded by an autosampler (Surveyor) onto a C18 trap column (inner diameter, 300 μm; length, 5 mm; particle size, 5 μm; LC Packings) for desalting and concentration

at a flow rate of 20 μl/min. Then, the trapped peptides were back flushed and separated on a homemade microcapillary column (length, 150 mm) packed with C18 (particle size, 5 μm) in 75-μm silica tubing (8-μm inner diameter orifice). The mobile phases, A and B, were composed of 0 and 80% acetonitrile, respectively, containing 0.1% formic acid. The gradient began at 5% B for 15 min, ramped to 20% B for 3 min, to 60% for 45 min, to 95% for 2 min, and, finally, to 95% B for 7 min. The column was equilibrated with 5% B for 10 min before the next run. The voltage applied to produce an electrospray was 2.5 kV, and the cone voltage was 30 eV. Argon was introduced as a collision gas at a pressure of 10 pounds per square inch. Data-dependent peak selection of the three most abundant MS ions from MS was used, where the collision energy was increased to 30 eV.

Database Search and Analysis—Peak lists were generated and processed using MassLynx software version 3.5 (Waters). MS spectra were smoothed once using a Savitzky Golary method set as ± 3 channels and centered using the top 50% of each peak. The resulting .dta files from each analysis were automatically combined into a single text file. The resulting peak lists were searched against National Center for Biotechnology Information (NCBI) non-redundant database 20051212 (taxonomy, human; entries, 103,913 human sequence entries) using Mascot search engine version 2.0 (Matrix Science). Mascot was used with monoisotopic mass selected, a precursor mass tolerance of ± 1.5 Da, and a fragment mass tolerance of ± 0.8 Da. Trypsin was selected as the enzyme, with one potential missed cleavage. ESI-QTOF was selected as the instrumental type. Oxidized methionine, pyroglutamate (N-term Q), propioamide cysteine, and carbamidomethylated cystein were chosen as variable modifications. With regards to acceptance criteria for protein identification, those candidates that were identified with 2 or more high scoring peptides from Mascot were selected. High score peptides corresponded to peptides that were above the threshold in Mascot searches ($p < 0.05$, peptide score > 40). Among the candidate proteins, one protein was singled out on the criteria that the theoretical pI and molecular mass closely match the estimated values on a two-dimensional gel and the sequence are more highly covered by the sequenced peptides. All peptide lists were compiled in supplemental Table I. In cases where multispots were identified to be one protein, the peptides of a protein identified with the highest score were listed. All the peptides were checked manually to see if they are found in proteins other than those searched in Mascot engine, and peptides common to different proteins were marked in italic. All identified proteins were checked to contain at least one specific and nonredundant peptide.

Northern Blot Analysis—Total RNA was isolated from the cultured cells using TRIzol (Invitrogen) and quantified spectrophotometrically. RNA samples were fractionated on a 1% formaldehyde agarose gel and transferred to a Hybond-N nylon membrane (Amersham Biosciences). cDNA fragments of the *MGAT5* gene were labeled with [α-^{32}P]dCTP using a Random Primer labeling kit (Stratagene) according to the manufacturer's instructions and hybridized with RNA blots using ULTRAhyb hybridization buffer (Ambion) overnight at 42 °C.

Western and Lectin Blot Analyses—Proteins were resolved on 10–15% SDS-PAGE gels and transferred electrically onto PVDF membranes (Immobilon-P, Millipore). The membranes were blocked in 0.05% Tween 20-TBS containing 5% skim milk (immunoblot) or 3% BSA (lectin blot) and then incubated with primary antibodies or biotin-labeled lectin. After hybridizing with horseradish peroxidase-labeled secondary antibody (Cell Signaling) or horseradish peroxidase-avidin conjugates (Vector Laboratories, Inc.), the membranes were reacted with ECL Western blotting detection reagents (Pharmacia) and exposed to X-ray film for 1–2 min.

Immunoprecipitation—Tissue samples were prepared from resection specimens from colon cancer patients at the Catholic University Hospital (Incheon, Korea) with the patients' agreements. Proteins

extracted in 50 mM Tris-HCl (pH 8.0), 5 mM EDTA, 150 mM NaCl, and 0.1% Nonidet P-40 were immunoprecipitated using monoclonal human TIMP-1 antibody (Santa Cruz Biotechnology). The precipitated complexes were denatured with SDS-PAGE loading buffer.

Protein Purification and Quantification—TIMP-1 was purified on an IgG$_{anti-TIMP-1}$-conjugated Sepharose 4B column, prepared by incubating a monoclonal TIMP-1 antibody (Santa Cruz Biotechnology) with CNBr-activated Sepharose 4B at 37 °C for 4 h according to the manufacturer's instructions. The protein concentration of the purified TIMP-1 was determined using a molar extinction coefficient of 26,500 M^{-1} cm^{-1}.

Tumor Cell Migration and Invasion Assay—Cell migration assays were performed using 12-well Transwell chambers (Corning Inc.) with 8 μm-pore size polycarbonate inserts as described previously (6). Cells migrating or invading to the lower surface of the filters were fixed in methanol, stained with Toluidine blue, and counted with a microscope at ×400.

In Vitro Gelatinase Inhibition Assays—The proforms of matrix metalloproteinase (MMP), ProMMP-2 and proMMP-9 (Calbiochem), were activated by incubation with an equal molar ratio of active MMP-3 (Sigma) at 37 °C for 4 h and 1 mM *p*-aminophenylmercuric acetate at 37 °C for 2 h, respectively. The active gelatinases were purified on a gelatin-Sepharose (Sigma) column according to the previous procedures (15). Following the incubation of gelatinases (50 ng) with equal molar ratio of TIMP-1 in 50 mM Tris-HCl buffer (pH 7.5), 150 mM NaCl, 5 mM CaCl$_2$, 0.1 mM ZnCl$_2$, 0.02% Brij-35, and MMP inhibitors at 4 °C for 1 h, fluorogenic substrates DABCYL-GABA-PQGL-E(EDANS)-AK-NH$_2$ (Calbiochem) was added at 8 μM, and the hydrolysis activity was kinetically measured in an LS 45 Luminescence Spectrometer (PerkinElmer Life Sciences) at an excitation and emission wavelengths of 338 and 495 nm, respectively.

Determination of Kinetic Parameters for TIMP-1-Gelatinase Interaction—Kinetic parameters (k_{on}, k_{off}, K_i) for TIMP-1-gelatinase interaction were determined according to the previous procedure (16) with minor modifications. Briefly, the first-order binding constants (k) were determined under the following conditions. Active gelatinases were added at 1 nM into the reaction mixture containing 8 μM fluorescent substrate and TIMP-1. TIMP-1:mock and TIMP-1:GnT-V were varied from 0 to 6 nM and 0 to 25 nM, respectively. Progress curves were recorded at 37 °C in an LS 45 Spectrometer (PerkinElmer Life Sciences). The curves were fitted to Eq. 1 (12):

$$[P] = \nu_s t + (\nu_0 - \nu_s)(1 - e^{-kt})/k \qquad \text{(Eq. 1)}$$

in which [P] is the product concentration, v_0 and v_s are the initial and steady-state velocities, respectively, and k is pseudo first-order rate constant of inhibition: v_s, and k were calculated with regression method using SigmaPlot (SPSS Science, Inc.). The second-order rate constant (k_{on}) was calculated by the linear regression of k as a function of TIMP-1 concentration.

The k_{off} values were estimated from the time course for the dissociation of the gelatinase-TIMP-1 complex. The complexes were prepared by incubation of equimolar amounts of gelatinases and TIMP-1 (1 μM) at 37 °C for 1 h. Complex dissociation was achieved by diluting the complexes 1,000-fold in a cuvette containing the substrate. After reaching equilibrium, the recorded time-response curves were fitted to Eq. 1. The negative of the obtained values were used as an approximation of k_{off}. The inhibition constants (K_i) were calculated by $K_i = k_{off}/k_{on}$.

Zymography—Latent and active forms of gelatinases were run on 12% SDS-PAGE gel copolymerized with 0.5% (w/v) gelatin and 5 μg/ml of recombinant protein (rTIMP-1) or the mutant proteins. Gelatinases and recombinant proteins in the gel were allowed to bind at 4 °C overnight, and the embedded gelatin was allowed to be hydrolyzed at 37 °C for 12 h in 50 mM Tris-HCl (pH 7.5), 150 mM NaCl, 5 mM CaCl$_2$, 0.1 mM ZnCl$_2$, and 0.02% (w/v) Brij-35 containing, if necessary,

gelatinases specific inhibitors or EDTA.

Profiling of N-Glycans of TIMP-1—Profiling of the *N*-glycans of TIMP-1 was performed as described previously (17) with minor modifications. Briefly, about 200 pmol of TIMP-1 purified either from WiDr:mock or WiDr:GnT-V was resolved on a 12% SDS-PAGE gel. The bands corresponding to TIMP-1 were sliced to pieces, washed with 50 mM NaHCO$_3$ buffer (pH 7.0) for 1 h, and dried *in vacuo*. In-gel digestion of *N*-glycans was performed for 18–24 h by treatment with 10 units of PNGase-F in 50 mM NaHCO$_3$ buffer (pH 7.0). The digested *N*-glycans were extracted from the gels on a vortexer twice with 100 μl of water and once with acetonitrile, and, if necessary, the extracted *N*-glycans were further deglycosylated with sialidase and β-galactosidase according to the manufacturer's instructions. Following desalting of the *N*-glycan samples on a graphitized carbon column (Alltech), *N*-acetylneuraminic acids on the glycans were esterified with iodomethane in anhydrous dimethyl sulfoxide at room temperature for 2 h. After unreacted iodomethane was vaporized under nitrogen stream, glycan samples were dried *in vacuo* and reconstituted in 2 μl of 25% acetonitrile. If necessary, glycan samples were desalted with Bio-Rex MSZ 501 (D) ion exchangers (Bio-Rad) prior to reconstitution. The reconstituted samples were mixed with equal volume of matrix consisting of saturated 2,5-dihydroxybenzoic acid and 6-aza-2-thothymine, and the mixtures were applied on a MALDI MSP 600/96 chip and dried in air. All mass spectra were acquired on a Bruker Daltonics microflex MALDI-TOF mass spectrometer (Bruker Daltonics) using FlexControl software version 2.4 and processed using Flexanalysis software version 2.4 to analyze raw data. Each spectrum was calibrated internally with angiotensin II (average mass of $[M+H]^+$: 1047.20 Da), angiotensin I (1297.51 Da), substance P (1348.66 Da), bombesin (1620.88 Da), ACTH clip 1–17 (2094.46 Da), ACTH clip 18–39 (2466.73 Da), and somatostatin 28 (3149.61 Da) to reach a typical mass measurement accuracy of ±23 parts/million in the 1400–4500 *m/z* range. All samples were irradiated with UV light (337 nm) from an N$_2$ laser. The neutral and sialylated *N*-glycans after esterification were analyzed at a 20-kV accelerating voltage in the reflectron positive ion mode in which glycans are observed as $[M+Na]^+$ ions. About 200 scans were averaged for each of the spectra. The *N*-glycan structures were deduced from the *m/z* values, which were blasted with a mass tolerance of 5 kDa against the Consortium for Functional Glycomics database (www.functionalglycomics.org).

RESULTS

TIMP-1 Is a Target Protein for GnT-V in Colon Cancer Cells—GnT-V is an enzyme that catalyzes the attachment of a β1,6-GlcNAc linkage to the core *N*-linked glycan (Fig. 1*A*). We have identified target proteins for GnT-V from secreted glycoproteins that bind to lens culinaris column (13). However, glycoproteins did not necessarily bind to the lectin column, which prompted us to search for target proteins in this study from total secretome of WiDr:mock cells that expresses GnT-V at very low, almost negligible levels and GnT-V overexpressing cells (WiDr:GnT-V) (Fig. 1*B*). We performed comparative two-dimensional electrophoresis and lectin blot analyses of the secreted proteins using L$_4$-phytohemagglutinin (L-PHA), a lectin that basically recognizes the β1,6-GlcNAc moiety (Fig. 1*C*). Spots displayed differentially between WiDr:mock and WiDr:GnT-V were sliced, tryptic-digested, and identified by mass spectrometry. Fig. 1*C* shows a representative result of several independent experiments. Some proteins from WiDr:mock cells contain a β1,6-GlcNAc linkage in
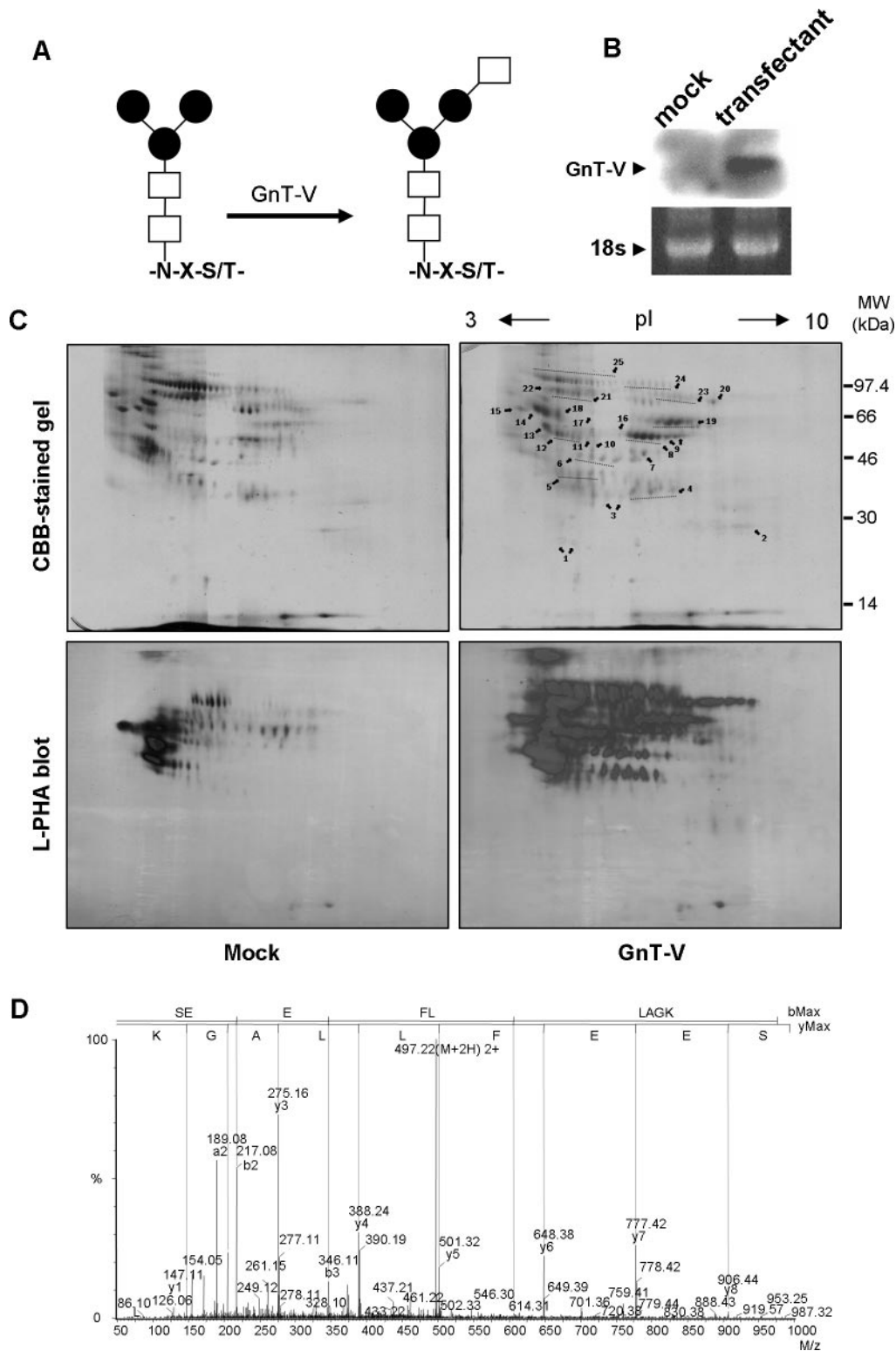
FIG. 1. **Search for target proteins of GnT-V in colon cancer WiDr cells and the identification of TIMP-1 as a candidate.** *A*, GnT-V-catalyzed addition of β1,6-GlcNAc to the core *N*-glycan comprised of GlcNAc ($\square$) and mannose (●). *N*, asparagine; *S*, serine; *T*, threonine; *x*, any amino acid except proline. *B*, WiDr colon cancer cells were transfected with the *MGAT5* gene, and the stable transfectant cells were established. *C*, protein samples prepared by precipitation of WiDr conditioned serum-free media were displayed on two-dimensional electrophoresis gel. *Spots* that displayed differentially between WiDr:mock and WiDr:GnT-V cells were used for identification. Proteins indicated by *arrows* were identified as follows; *1*, heparan sulfate proteoglycan perlecan; *2*, tissue inhibitor of metalloprotease-1; *3*,

TABLE I

Proteins differentially recognized by L-PHA on 2-DE gels and identified by ESI-MS spectrometry and a Mascot blast search against NCBInr

Accession gi no.	Identities	Peptides matched	Sequence coverage (%)	Total score[a]	M_r/pI[b]	Levels[c] ($\pm$S.D.)
177836	α-1-antitrypsin precursor	7	26.3	438	46.7/5.5	0.26 (0.03)
15079348	Angiotensinogen preproprotein	3	10.1	189	53.1/5.8	1.19 (0.07)
4261632	β-N-acetylhexosaminidase A	10	22.3	575	60.7/5.0	1.77 (0.17)
54697170	Cathepsin D preproprotein	5	11.7	320	44.5/6.1	3.87 (0.24)
3650498	Cathepsin X precursor	2	5.9	107	33.9/7.1	1.19 (0.11)
68533097	DDR1 variant protein	3	4.4	141	99.0/6.3	0.66 (0.06)
16877430	Dipeptidyl peptidase 7 preproprotein	3	11.3	146	54.3/5.9	2.33 (0.17)
38327632	Discoidin receptor tyrosine kinase	2	6.1	99	96.9/6.1	1.40 (0.12)
4758116	Dystroglycan 1 precursor	2	3.3	106	97.6/8.7	1.42 (0.15)
5031863	Galectin 3 binding protein	3	6.8	147	65.3/5.1	0.53 (0.06)
4504151	Granulin isoform 1 precursor	3	5.7	149	63.5/6.4	1.21 (0.09)
5729877	Heat shock 70 kDa protein 8 isoform 1	7	14.6	379	70.9/5.4	2.47 (0.15)
15010550	Heat shock protein gp96 precursor	9	12.0	484	90.2/4.7	0.34 (0.04)
11602963	Heparan sulfate proteoglycan perlecan	3	1.1	171	466.6/6.0	3.26 (0.33)
16924217	Hexosaminidase B preproprotein	5	10.4	266	63.1/6.3	0.87 (0.06)
5080756	Human Fc binding protein	3	1.6	179	572.1/5.1	0.19 (0.02)
106586	Ig kappa chain V-III	3	25.1	252	23.1/5.8	1.48 (0.11)
9845498	Laminin γ1 precursor	11	8.7	746	177.6/5.0	1.47 (0.06)
56682964	Legumain preproprotein	3	12.7	152	49.4/6.1	1.54 (0.11)
51095116	Met proto-oncogene	7	5.3	471	155.4/7.0	1.76 (0.04)
4503899	N-acetylgalactosamine-6-sulfatase	5	14.9	295	58.0/6.3	0.63 (0.06)
4504061	N-acetylglucosamine-6-sulfatase	8	17.9	457	62.0/8.6	0.18 (0.02)
57209715	Prosaposin	5	10.9	318	58.1/5.1	2.01 (0.08)
4505989	Protective protein for β-galactosidase	2	5.4	178	54.5/6.2	0.35 (0.04)
2136061	Protein-tyrosine kinase-related receptor PTK7	7	9.2	432	118.3/6.7	0.47 (0.02)
57160745	Protein tyrosine phosphatase kappa	7	7.8	374	162.0/5.6	2.04 (0.07)
5231228	Ribonuclease T2 precursor	5	25.3	262	29.5/6.7	0.86 (0.07)
57210053	Tissue inhibitor of metalloproteinase-1	4	26.1	215	23.2/8.5	1.97 (0.06)
120749	Tumor-associated calcium signal transducer 1	2	11.8	184	34.9/7.4	1.08 (0.09)
38026	Zn-α-2-glycoprotein	4	19.5	234	34.7/5.7	0.41 (0.05)

[a]Total score is a sum of the score values obtained from each of an individual peptide. Score is $-10 \times$ Log (P), where P is the probability that the observed match is a random event; it is based on NCBInr database using the MASCOT searching program as MS/MS data.

[b]Molecular weight (M_r) and isoelectric point (pI) are theoretical values where glycan residues were not considered for the calculations. The theoretical values are prone to be changed by an attachment of glycans to peptides and thus to be different from the experimental values estimated on two-dimensional electrophoresis gels.

[c]Numbers refer to the relative levels of each protein from WiDr:GnT-V compared to those from WiDr:mock ($n = 5$).

N-linked glycans, suggesting that the β1,6-GlcNAc linkage on the protein molecules was acquired during cancer development of a normal cell, or the linkage is a cognate component in itself that is essential for either functional or structural integrity. In contrast, proteins from WiDr:GnT-V were more reactive to L-PHA compared with those from WiDr:mock. This may arise from a net increase in the β1,6-GlcNAc glycan moiety without any significant change in expression level, from simply the up-regulation of otherwise undetectable glycoproteins with a cognate β1,6-GlcNAc linkage, or from simultaneous increases in the β1,6-GlcNAc glycan moiety and protein levels. The identified proteins in several sets of independent experiments are compiled in Table I. To minimize the possibility of systematic errors, the proteins that were exactly matched to at least two unique peptides with significant score values ($p < 0.05$) and no miss were screened. Some proteins showed multispots, which is a common feature of some glycoproteins, and in this case, the lowest score values are

ribonuclease T2 precursor; *4*, cathepsin X precursor; *5*, Zn-α-2-glycoprotein; *6*, cathepsin D preproprotein; *7*, protective protein for β-galactosidase; *8*, legumain preproprotein; *9*, human Fc binding protein; *10*, discoidin receptor tyrosine kinase; *11*, angiotensinogen preproprotein; *12*, α-1-antitrypsin precursor; *13*, β-N-acetylhexosaminidase A; *14*, prosaposin; *15*, galectin 3 binding protein; *16*, N-acetylgalactosamine-6-sulfatase; *17*, dipeptidyl peptidase 7 preproprotein; *18*, heat shock 70 kDa protein 8 isoform 1; *19*, hexosaminidase B preproprotein; *20*, granulin isoform 1 precursor; *21*, N-acetyl-glucosamine-6-sulfatase; *22*, heat shock protein gp96 precursor; *23*, DDR1 variant protein; *24*, protein-tyrosine kinase-related receptor PTK7; *25*, protein tyrosine phosphatase κ. *D*, peptide derived from *spot 2* in *panel C* was sequence analyzed by ESI/Q-TOF mass spectrometry, blasted against the Mascot database, and identified to be human TIMP-1 from the sequence SEEFLIAGK seen in the mass spectrum together with other sequences.

shown in Table I. All the proteins in Table I were confirmed by an independent, the more direct approach: protein samples were reduced by β-mercaptoethanol to minimize the possibility of "junk proteins" interacting with the glycoproteins and were thereafter subject to desalting to remove β-mercaptoethanol. Precleared with avidin-agarose beads, the reduced proteins were allowed to interact with L-PHA-avidin-agarose beads. After intensive washing, the bound proteins were completely denatured in an SDS-PAGE denaturation buffer, resolved on a minimal size of SDS-PAGE gels, and digested in gel by trypsin. The tryptic peptides were eluted out and sequence analyzed with an LTQ-FTICR (7 Tesla) mass spectrometer equipped with a nanoelectrospray ion source. Blast search was carried out as described in "Experimental Procedures." The identified proteins that derived from WiDr:GnT-V but not WiDr:mock and the related information are available in supplemental Fig. 1. Fig. 1D shows a representative peptide sequence of TIMP-1 as determined by ESI/Q-TOF and a Mascot blast search program.

Changes in the serum level of proteins associated with diseases are of great interest in biomarker discovery, and glycoproteins constitute a significant portion of serum proteins. In this regard, the levels of proteins in the WiDr-conditioned RPMI 1640 media were also investigated using the differential in-gel electrophoresis method. Proteins from WiDr:mock and WiDr:GnT-V were labeled with cy3- and cy5-fluorescent dyes, respectively, resolved on two-dimensional gels, and the fluorescent intensities of each spot were measured. supplemental Fig. 2 shows a representative result of five independent experiments. Some of the glycoproteins show multispots on a two-dimensional electrophoresis gel, and even a glycoprotein of the same protein identity were not overlapped at least in our case, where the glycan changes result in a shift in migration on a gel. Thus, each spot was reidentified by mass analysis after quantification. As noted in Table I, many of the proteins show an increased level in GnT-V overexpressing cells, while some proteins were either decreased or did not show any dramatic alteration. Both changes in glycan structure and the altered levels of the proteins, as described in Table I, could provide an important clue for further study in which the candidate proteins could be validated in human blood or proximal biofluids.

TIMP-1 is an endogenous inhibitor of MMPs that play a critical role in cancer cell invasion and migration and has been reported to be implicated in the malignant transformation of cancer cells in some manner (18). For this reason, TIMP-1 was chosen as a model glycoprotein to show how an aberrant glycosylation induced by GnT-V affects cancer progressions and malignancy, and it was hypothesized that, at least in part, the pathological symptoms manifested by the action of GnT-V result from an alteration in the N-glycan structure of TIMP-1.

Establishment of Stable Transfectants of TIMP-1 and the Glycosylation Mutants—To examine the effects of GnT-V-initiated alterations of N-linked glycans on TIMP-1 on cancer cell behavior, site-directed mutageneses were performed in which either or both of Asn[30] and Asn[78] were replaced with Gln (Fig. 2A). Together with the wild-type *TIMP-1* gene, the three mutated genes were transfected into cells and designated as T-N30Q, T-N78Q, and T-N30/78Q. The repetitive transfections and selections were conducted so as to meet two requirements: the first is that the amounts of TIMP-1 recombinant protein (rTIMP-1) secreted are as much as possible so as to minimize the effects of cognate TIMP-1. The other is that the amounts of rTIMP-1 proteins secreted are equal among the transfectants in order to exclude the differences in cancer cell behavior arising from difference in the levels of secreted TIMP-1. Stable transfectants satisfying both requirements were selected based on an immunoblot analysis (Fig. 2B). The secretion level of cognate TIMP-1 was 18.4 $\pm$ 0.8% of that for rTIMP-1 in WiDr:GnT-V cells and negligible in case of WiDr:mock cells as assessed by using Quantity One software program (Bio-Rad). The molecular mass of the mature form of TIMP-1 is ~28.5 kDa, of which N-linked glycans account for about 8 kDa (19). The eradication of either of the two N-linked glycosylations produced rTIMP-1 mutant proteins whose molecular masses were reduced by 4 kDa, confirming that the intended transfectant cells were produced.

To deduce the structure of aberrant glycan of TIMP-1, the cognate TIMP-1 was purified both from WiDr:mock and WiDr:GnT-V and subjected to two-dimensional electrophoresis followed by immunoblot using an anti-TIMP-1 antibody or a lectin blot analysis using L-PHA and *Datura stramonium* agglutinin (DSA), a lectin recognizing lactosamine moiety (Fig. 2C). TIMP-1 from WiDr:mock was divided into one main spot in the basic region and two minor ones in the acidic region on two-dimensional electrophoresis gels, indicating that only small fraction of TIMP-1 possibly carries an acidic glycosyl residue such as sialic acid. None of the subdivisions carried β1,6-GlcNAc or lactosamine linkages. However, the majority of the aberrant TIMP-1 showed β1,6-GlcNAc linkages and extended polylactosamine glycan moieties. Moreover, TIMP-1 was divided into multispots on two-dimensional electrophoresis gels, showing an increment of heterogeneity. Taken together, TIMP-1 aberration is characterized by the attachment of β1,6-GlcNAc linkages, polylactosaminylation, and an increase in terminal elaborations with acidic residue. Besides, it appears that the secretion level of TIMP-1 is elevated upon the attachment of aberrant N-glycan (Fig. 2B).

Mass analysis of N-glycans of TIMP-1 was performed on a MALDI-TOF mass spectrometer (Fig. 3A). The N-glycan structures were deduced from the *m/z* values of the detected ions, which were blasted against the Consortium for Functional Glycomics database, and the most relevant composition of the monosaccharide building blocks were assigned. The heterogeneous N-glycans of TIMP-1 from WiDr:mock were resolved in the range of 1500–3500 *m/z*, all of which were deviated from the calculated value (~4 kDa), consistent with the previous measurement (20). Overall, the average mass of
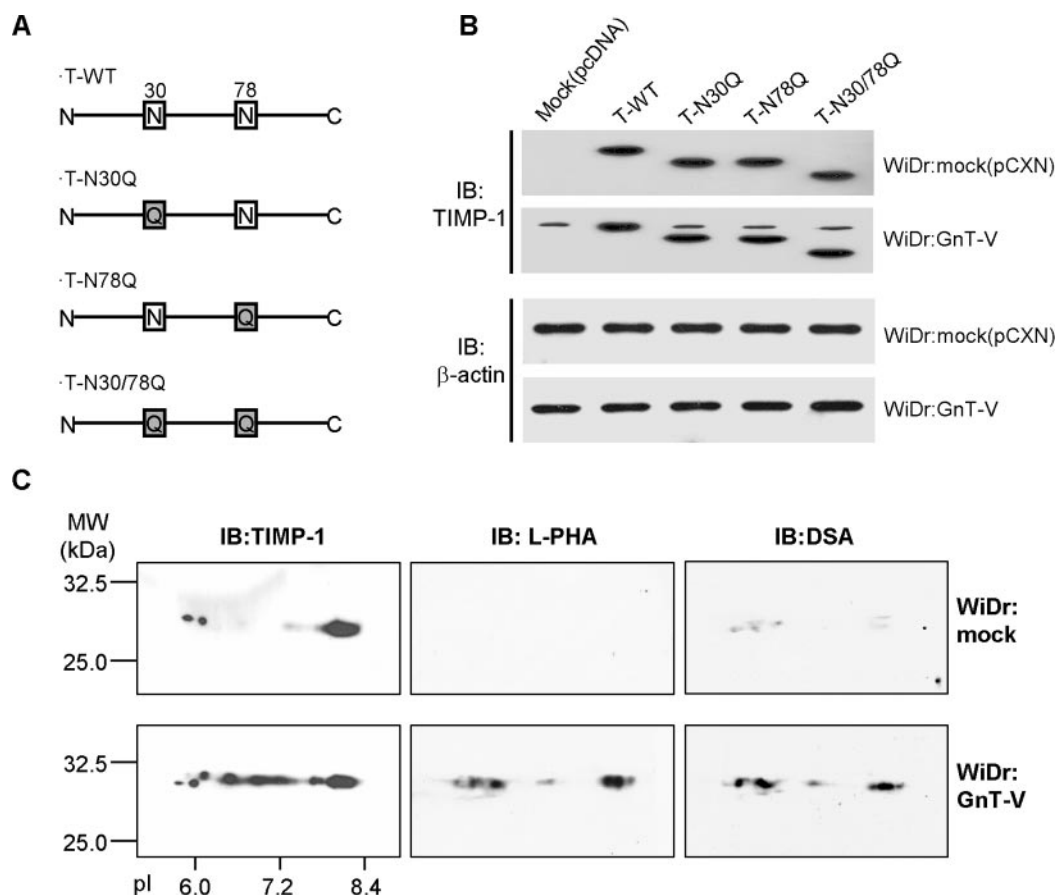
FIG. 2. **Establishment of stable transfectants of TIMP-1 and the glycosylation mutants.** *A*, wild-type *TIMP-1* and three glycosylation mutant genes were cloned. *B*, the cloned genes were transfected into WiDr:mock and WiDr:GnT-V cells, and the stable transfectants expressing equal amounts of the recombinant proteins were selected. *C*, the structure of the aberrant glycan on TIMP-1, initiated by the GnT-V-catalyzed attachment of β1,6-GlcNAc, was deduced by two-dimensional electrophoresis combined with lectin and immunoblot (*IB*) analyses. β1,6-GlcNAc and additional polylactosamine moieties could be deduced from the L-PHA and DSA blot, respectively, in aberrant TIMP-1 molecules. *MW*, molecular mass.

N-glycans of TIMP-1 from WiDr:GnT-V was higher than that from WiDr:mock, and the GnT-V-catalyzed TIMP-1 showed the more heterogeneous profiling of *N*-glycans. Interestingly, the masses of some *N*-glycans of TIMP-1 from WiDr:GnT-V were calculated to differ by ~1035 *m/z*. That is, mass values of peaks at 1809, 2421, and 3353 *m/z* in WiDr:mock match those peaks at 2847, 3458, and 4388 *m/z*, respectively, when the increment value is subtracted. Considering an increment in mass during esterification of *N*-acetylneuraminic acid (Neu), the increment value corresponds to the molecular mass of adducts, $Neu_1Gal_2GlcNAc_2$. Upon *N*-acetylglucosaminylation, galactose (Gal) and GlcNAc were alternatively added, and terminal Neu was then decorated. It is, however, not clear whether the glycan of 4127 *m/z*, marked with asterisk (*), was derived from that of 2785 *m/z* by gaining another sialic acid or if it was derived from another glycan substrate, possibly ~3092 *m/z*, and the glycan of 3092 *m/z* was not detected in the profiling of *N*-glycans from WiDr:mock. Two repeats of lactosamine residues on the adducts are thought to confer reactivity toward the DSA lectin, and Neu residues produce the hetero-

geneous behaviors on two-dimensional electrophoresis gels. Indeed, *N*-glycans from WiDr:mock are neutral or contain 2 Neu residues, whereas those from WiDr:GnT-V have various numbers (0–4) of Neu residues. The composition of the annotated glycans in Fig. 3*A* was confirmed by a mass analysis of each glycan that had been treated with sialidase (Fig. 3*B*) and sialidase plus β-galactosidase (Fig. 3*C*). For example, the glycan with *m/z* 2785 from WiDr:mock was estimated to be reduced to $Gal_3Man_3GlcNAc_5Fuc_1$ (*m/z* 2176) by the loss of two residues of Neu when treated with sialidase, which were, in turn, further processed to $Man_3GlcNAc_5Fuc_1$ (*m/z* 1690) by treatment with β-galactosidase and sialidase.

Effects of the Aberrant Glycosylation of TIMP-1 on In Vitro Cell Migration and Invasion—Cumulative studies indicating that an increase in GnT-V activity correlates with the high invasive/metastatic potential of cancer cells and the fact that TIMP-1 is associated with the potential prompted us to examine the role of *N*-linked glycosylation of TIMP-1 in the metastatic potential of colon cancer cell. For this, the migra-
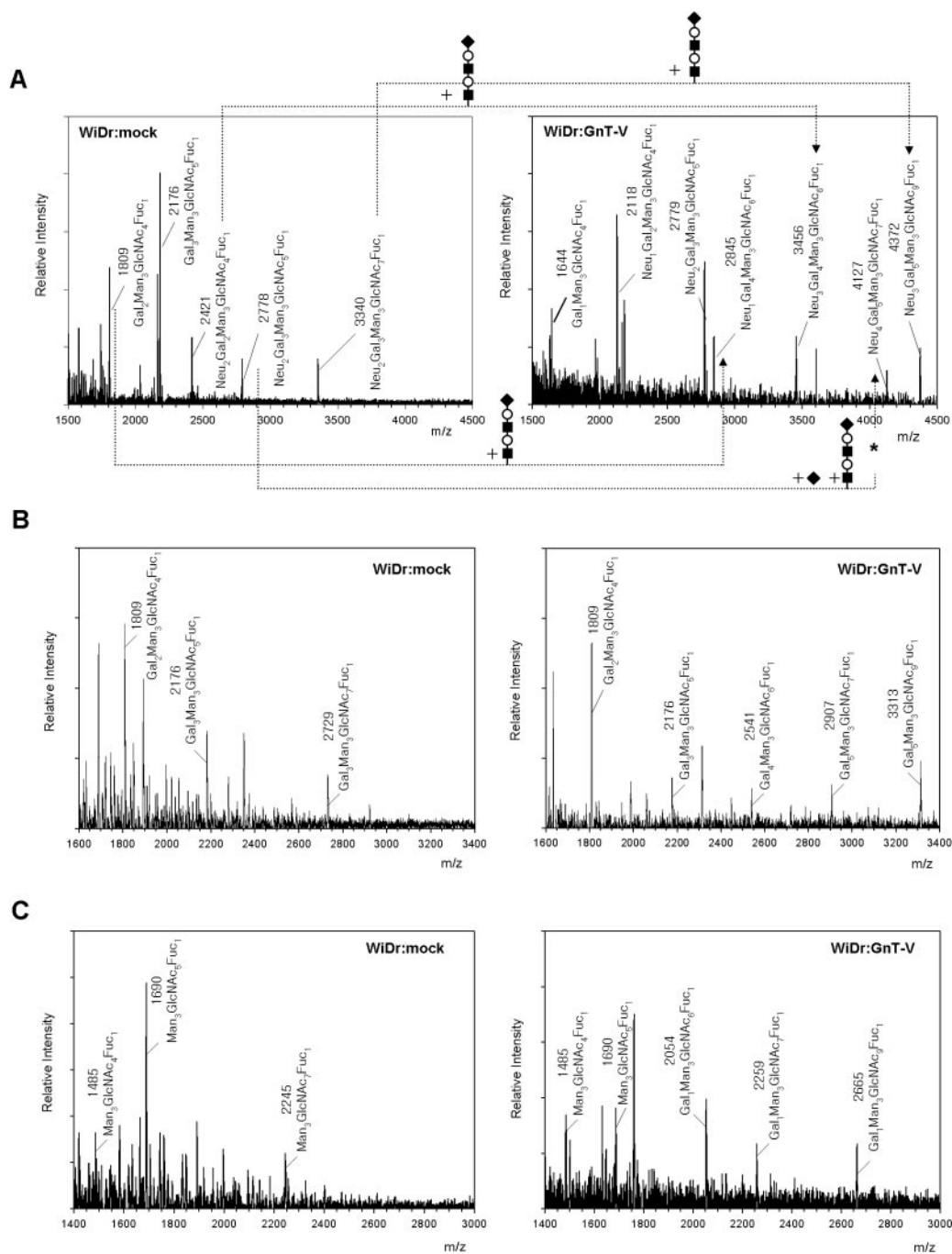
FIG. 3. **Profiling of *N*-glycans of TIMP-1 in WiDr cells.** *A*, profiling of TIMP-1 glycans from WiDr:mock and WiDr:GnT-V was performed. Glycans digested with PNGase F were mass analyzed in a MALDI-TOF mass spectrometer, and the composition of each glycan was deduced from the mass value. The annotated composition was confirmed by treatment with sialidase (*B*) and *β*-galactosidase plus sialidase (*C*). ■, *N*-acetylglucosamine; ○, galactose; ♦, *N*-acetylneuraminic acid.

tion and invasion properties of each TIMP-1 transfectant were investigated *in vitro*. Concerning cell migration, GnT-V affected cell migration, but in a TIMP-1-independent manner (Fig. 4*A*). Little difference in the motility was observed among the TIMP-1 transfectants of WiDr:mock cells as well as WiDr:GnT-V cells. However, GnT-V conferred a higher motility on WiDr cells irrespective of the mutational status of TIMP-1,

indicating that the increment of cell motility is actually aided by GnT-V but possibly mediated by other mediator proteins or through a signal transduction pathway independent of TIMP-1 as reported previously (6).

Meanwhile, glycan moieties on TIMP-1 affected the cell invasion significantly (Fig. 4*B*). T-N30/78Q:GnT-V cells showed a dramatically slow cell invasion compared with T-WT:GnT-V,
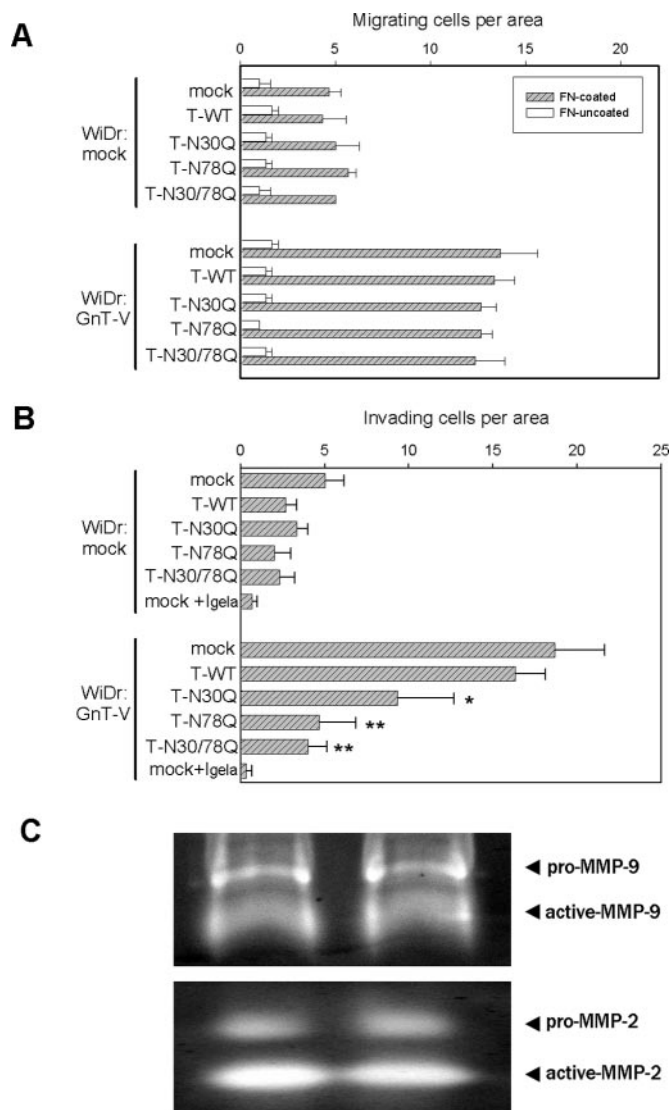
FIG. 4. **Effects of the aberrant glycosylation of TIMP-1 on cell migration and invasion.** Cells (2×10^4) were allowed to migrate in RPMI 1640 medium plus 0.1% BSA containing, if necessary, gelatinases inhibitor (*Igela*) for 4 h (*A*) and a Matrigel-coated 24-well Boyden chamber for 22 h (*B*), and cells that migrated to the lower surface of the filters, some of which were precoated with fibronectin (*FN*) (25 μg/ml), were counted. The values are the means of three independent experiments with standard deviations (*, $p < 0.05$; **, $p < 0.01$). *C*, MMP-2 and MMP-9 were retrieved from WiDr conditioned RPMI 1640 media containing 10% FBS. MMP-2 was immunoprecipitated using anti-MMP-2 monoclonal antibody, and MMP-9 was partially purified on a Con A-agarose column. Gelatin zymography was performed on 10% SDS-PAGE gel with 0.5% (w/v) gelatin copolymerized.

and T-N30Q and T-N78Q were intermediate between them (Fig. 4*B*). However, little difference was found among the TIMP-1 transfectants of WiDr:mock cells. Collectively, these data strongly suggest that aberrant TIMP-1 glycosylation, but not glycosylation itself, affects *in vitro* cell invasion.

In vitro cell invasion involves two distinct processes: the hydrolysis of basement membranes coated throughout the

8-μm pores and migration through the pores. Since no difference in cell migration itself was observed (Fig. 4*A*), we reasoned that the different cell invasion originated from differences in the hydrolysis rate of basement membrane. Treatment with gelatinase inhibitors significantly nullified the invasiveness of WiDr cells (Fig. 4*B*), indicating the involvement of hydrolysis of the basement membrane catalyzed by MMP-2 and/or MMP-9 (21, 22). In view of the result that the cell invasion rate was nearly the same among mock cells of TIMP-1 transfectant (Fig. 4*B*), the possibility that the differences in cell invasion could arise from the changes in the gelatinases-inhibitory ability of TIMP-1 induced by depletion of *N*-linked glycosylation of TIMP-1 was eliminated. Removal of the carbohydrates from human TIMP-1 by treatment with *N*-glycosidase F has been shown to have no measurable effect on the inhibitory activity (19). A difference in the migration and invasion rate between WiDr:mock and WiDr:GnT-V did not arise from a different expression of MMP-2 and MMP-9 (Fig. 4*C*); moreover, the transfection of TIMP-1 or the mutant gene did not alter the expression pattern of gelatinases (data not shown). Taken together, the results suggest that the aberration in TIMP-1 affects its inhibitory ability toward gelatinases and thus the rate in the hydrolysis of Matrigel coating materials. An increase in the hydrolysis rate through the aberration of TIMP-1 would eventually lead to the enhanced invasiveness of WiDr cells.

Effects of the Aberrant Glycosylation of TIMP-1 on Gelatinases Inhibition—To confirm that the TIMP-1 aberration results in mitigated inhibition on gelatinases, the proteolytic activities of active gelatinases were monitored in the presence of various gelatinase inhibitors. Gelatinase activities were kinetically monitored using fluorogenic substrate DABCYL-GABA-PQGL-E(EDANS)-AK-NH$_2$. When gelatinases were pre-incubated with equal molar ratios of TIMP-1, the steady state of the hydrolysis reaction reached directly after initiation with the pattern of nearly zero-order kinetics (inset of Fig. 5, *A* and *B*). The slope of formation of fluorescent products was used to determine the relative activity of gelatinases.

Consistent with previous reports (19, 23), our results showed that the depletion of the cognate *N*-linked glycans on TIMP-1 has little effect on gelatinase inhibition (Fig. 5, *A* and *B*). Rather, the aberrant glycans were responsible for the mitigated inhibition on gelatinases. rTIMP-1 and the mutant proteins purified from WiDr:mock retained wild-type levels of inhibitory activity, whereas T-WT from WiDr:GnT-V showed a significant loss of gelatinase inhibition.

The inhibition of gelatinases by TIMP-1 was confirmed by gelatin zymography (Fig. 5*C*), where the gelatinolytic ability of the latent and active forms of MMP-2 and MMP-9 were measured in the presence of various inhibitors. We reasoned that, if TIMP-1 is covalently incorporated in gelatin copolymerized gels, it could tether gelatinases in the vicinity, thereby inhibiting the gelatinolytic activity. The results show that rTIMP-1 isolated from WiDr:mock cells retained an inhibitory effect on
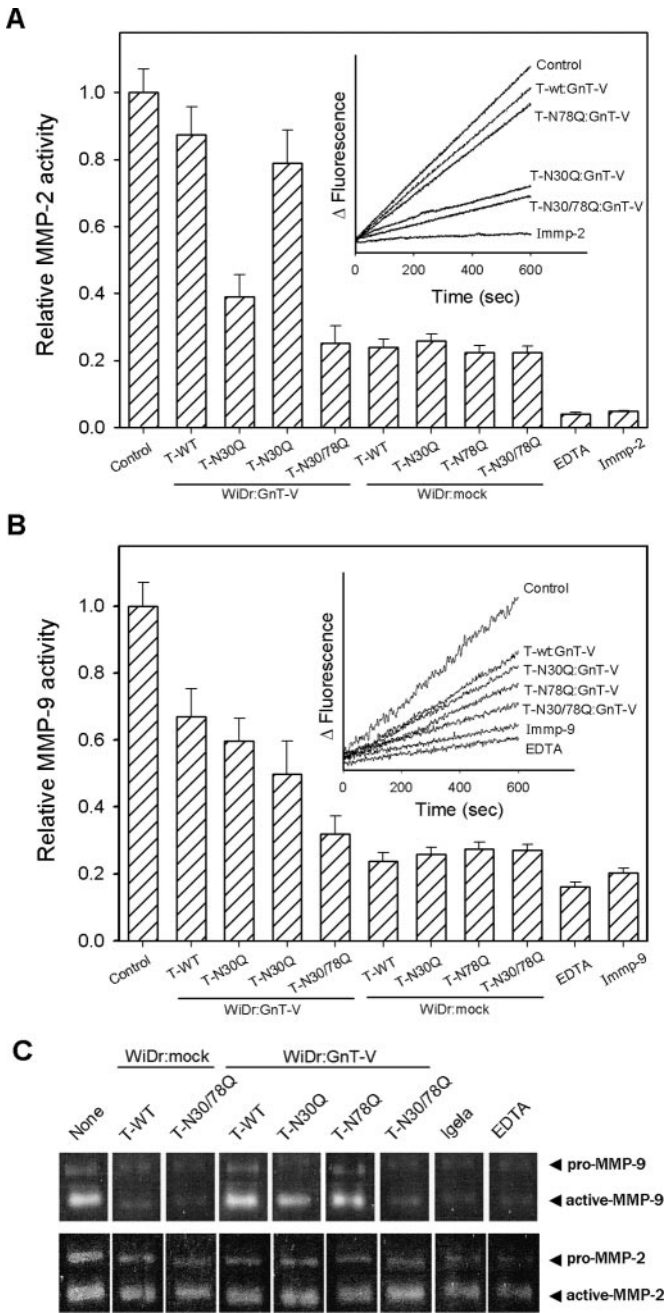
A

B

C

Fig. 5. **Effects of the aberrant glycosylation of TIMP-1 on gelatinase inhibition.** Following the incubation of gelatinases with the various inhibitors at 4 °C for 24 h, hydrolytic reactions of gelatinase A/MMP-2 (*A*) and gelatinase B/MMP-9 (*B*) were initiated at 37 °C by adding a fluorogenic substrate. Time courses of the activities were traced, and the slope at steady state was used for the relative activity. Immp-2 and Imp-9 refer to specific inhibitor for MMP-2 and MMP-9, respectively. *C*, effects of aberrant glycans of TIMP-1 on gelatinolytic activity of gelatinases were investigated by gelatin-zymography as described under "Experimental Procedures."

both the latent and active forms of MMP-9. rTIMP-1 from T-WT:GnT-V failed to tightly inhibit the gelatinolytic activity by MMP-9. The pattern of inhibition of MMP-2 by TIMP-1 was

not identical to the invasion assays and the fluorogenic assays, which might be due to restricted interactions of TIMP-1 and MMP-2 in gels. Nevertheless, rTIMP-1 from T-WT:GnT-V showed mitigated inhibition on MMP-2 compared with rTIMP-1 from T-Q30/78G:mock. These results suggest that the aberrantly attached glycans play a role as interferences in the TIMP-1 inhibition on the gelatinases.

Effect of Aberrant Glycosylation of TIMP-1 on Interaction with Gelatinases—To address the question of why the aberrant glycosylation of TIMP-1 results in a significant loss of gelatinase inhibition, we investigated the binding properties of TIMP-1 and gelatinases. The binding shows slow, tight-binding competitive inhibition and exhibits time-dependent inhibition (16) and, as a result, gelatinase activities over time showed a curvilinear function on the progress curves. Supplemental Fig. 3, *A* and *B* show the time courses for MMP-2 activity in the presence of various concentrations of TIMP-1: mock and TIMP-1:GnT-V, respectively. The kinetic pattern for MMP-9 was similar to that for MMP-2 (supplemental Fig. 4). Kinetic parameters (k_{on}, k_{off}, K_i) for gelatinase inhibition by TIMP-1 were calculated as described in "Experimental Procedures" and are compiled in Table II.

Kinetic parameters (k_{on}, k_{off}, K_i) for gelatinase inhibition by TIMP-1 were previously reported with some variations (16, 24–26). Olson *et al.* (16) attributed the variations to differences in the concentration of proteins and substrate. This taken into account, our data are not significantly different from previously reported values. As expected, the aberrantly glycosylated TIMP-1 was found to loosely bind to active gelatinases with a lower k_{on} and to dissociate more efficiently as assessed by the higher k_{off}. K_i for aberrant TIMP-1/gelatinases interactions was found to show 7.2-fold higher value than that for wild-type TIMP-1/MMP-2. The increase in inhibition constant was more dramatic for the TIMP-1/MMP-9 interaction, with the K_i being increased by 11.4-fold. These results indicate that the TIMP-1 aberration leads to a shift in equilibria for the TIMP-1/gelatinases interactions toward the dissociation process of the complex molecules. As a result, the tight binding and control of active gelatinases by TIMP-1 is loosened, resulting in a higher bioavailability of uncomplexed, uninhibited, free gelatinases.

Relations of TIMP-1 Aberration with Colon Cancer Invasion and Metastasis—The relationships between TIMP-1 aberration and cancer progressions has not been defined yet, but both *in vitro* experiments provided sufficient circumstantial evidence for an association of the aberration in cancer progression of colon cancer patients. To deduce the involvement of the aberrant glycosylation of TIMP-1 in colon cancer, both normal and tumor tissues of colon cancer cases were analyzed in terms of expression level and TIMP-1 glycosylation.

As is seen in Fig. 6*A*, the expression level of TIMP-1 did not reflect the progression of colon cancer. TIMP-1 expression was elevated in almost all colon cancers compared with its paired normal tissues consistent with previous reports (18,

TABLE II

Inhibition constants for active gelatinase/TIMP-1 interactions

TIMP-1	Gelatinases	k_{on} (M^{-1}·s^{-1}×10^5)	k_{off} (s^{-1}×10^3)	K_i (nM)
TIMP-1: mock	62kDaMMP-2	4.99 ± 0.72	2.71 ± 0.47	5.43 ± 1.39
	82kDaMMP-9	7.07 ± 0.64	2.26 ± 0.43	3.20 ± 1.23
TIMP-1: GnT-V	62kDaMMP-2	0.98 ± 0.06	3.83 ± 0.24	39.1 ± 8.38
	82kDaMMP-9	0.75 ± 0.07	2.74 ± 0.39	36.5 ± 6.54

27–30) and Fig. 2*B*, but the extent of the elevation was independent of Astler-Coller colon cancer stages, an index of colon cancer progression and commonly a metastatic parameter. Rather, at the stages where cell invasion and spreading to near tissues is prosperous, *i.e.* Astler-Coller grade C and D, an aberrantly glycosylated TIMP-1 was found in more than 70% of the colon cancer tissues tested, which is quite different from the case of *Group I*. Interestingly, the transcription level of GnT-V was estimated by RT-PCR to be increased in a cancer stage-dependent manner and concomitantly with the promotion of TIMP-1 aberration. When GnT-V overflows by a signal under cancerous conditions, the transferase is likely to promote TIMP-1 aberration and thus cancer malignancy.

Fig. 6*B* shows the representative results for 10 cases. Cases *1*, *4*, and *5* showed a marked increase in β1,6-GlcNAc-attached aberration in TIMP-1 glycosylation and, in agreement with Fig. 2*C*, a slight increase in molecular mass. Those cases showed an elevated transcription of GnT-V (Fig. 6*C*), a relatively high cancer stage and a clinically high tumor invasion to remote sites, especially metastasizing to regional lymph nodes (data not shown).

To our knowledge, the aberrant glycosylation of TIMP-1 has not been reported to correlate with the cancer invasion and metastasis *in vivo* or *in vitro*. Our data strongly suggest that the aberrant glycosylation of TIMP-1 induced by GnT-V is closely associated with the elevated invasion/metastasis potential in colon cancer cells.

DISCUSSION

A tumor-associated biomarker serves as an index that enables us to predict ongoing cancerous conditions and the progression of cancer by showing a difference in a quantitative or qualitative pattern. It is obvious that the current techniques for the biomarker discovery have focused on the quantitative aspects, that is, a differential expression level in cancer. A large body of data describes the correlation of a change in the quality of proteins, *i.e.* protein glycosylation, phosphorylation, and acetylation, with various diseases. In this report, we suggest that a consideration of the qualitative aspects of TIMP-1 provides the more accurate diagnostic and prognostic information on colon cancer when integrated with the data on the expression level. One of the intriguing features is that TIMP-1 has seemingly discordant, dual functions; TIMP-1 not only inhibits cancer progression by abrogating MMPs but also has effects on cancer cell growth and survival in an MMP-dependent or -independent manner. What would

happen if the level of TIMP-1 is maintained at a high level? It would control MMPs quite efficiently so that cancer progression might never occur or be retarded. Actually, the overexpression of TIMP-1 inhibits tumor growth and metastasis of melanoma (31) and suppresses the metastatic potential of human gastric cells (32) and oral squamous cell carcinoma (33). However, this is quite contradictory to reports that TIMP-1 is up-regulated in many cancer types (18, 27–30) and the reports that a high level of TIMP-1 correlates with a poor prognosis (34, 35). Moreover, high preoperative plasma TIMP-1 levels are associated with a short survival of patients with colorectal cancer (36), lung cancer (37), and gastric cancer (38). If the effects of TIMP-1 on cancer development and progression are taken into account only in terms of "quantity" without consideration of "quality," incessant debates over the genuine role of TIMP-1 in biological systems would occur and, although both aspects are relevant, it would fail to clearly explain whether TIMP-1 is pro-oncogenic or not. Here we suggest a plausible compromise to this "paradox." Tumor onset occurs in the early stage, and cell growth and anti-apoptotic activity are required at that stage. The higher level of TIMP-1 meets this requirement, and *N*-glycosylation of TIMP-1 would exert no effect on this tumor onset. Consistent with this suggestion, it has been demonstrated that TIMP-1 has a significant tumor stimulating effect during tumor onset (39) but suppresses tumor growth during the late state of tumor progression (40). However, it is likely that the "reins" that have sequestered tumor progression are slackened via an acquired aberrancy of TIMP-1 glycosylation upon the onset of the communication with GnT-V (supplemental Fig. 5). This implies that, although TIMP-1 levels are maintained at a high level or increase further, TIMP-1 levels were elevated by GnT-V, the net direction of cancer phase would be oriented toward cancer progression, and the turning point toward cancer progression may be associated with the interplay of TIMP-1 and GnT-V. An overexpression of TIMP-1 inhibits invasion and metastasis ((31, 32, 41); Fig. 4*B*), but the coexpression of TIMP-1 with GnT-V, previously unreported, nullified such inhibitory effects (Figs. 4 and 5). It is likely that GnT-V affects tumor progression mainly through TIMP-1 aberration, although another collateral mechanism is also possible (5–7).

TIMP-1 binds noncovalently to catalytically active MMP-2 and MMP-9 with a 1:1 stoichiometry and a dissociation constant ~10^{-8} M. Indeed, the values are true for the interactions of normal TIMP-1 with gelatinases. Our biochemical data indicate that the aberration of TIMP-1 leads to a decrease in
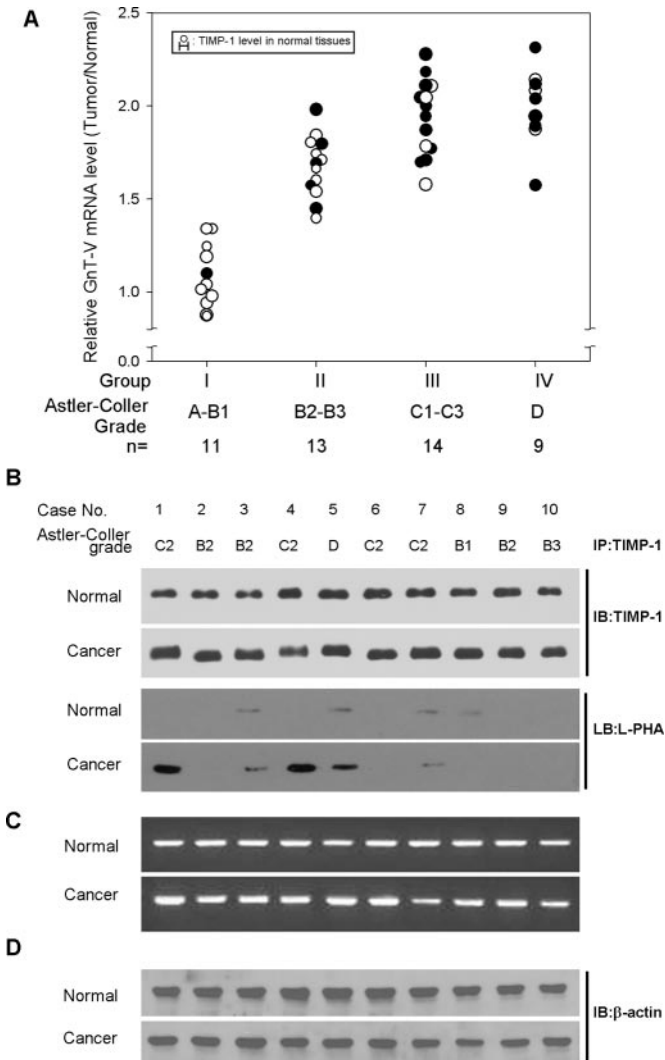
FIG. 6. **Correlation of TIMP-1 aberration with colon cancer progression.** *A*, the normal tissues and cancer tissues from colon cancer cases of each stage were compared with respect to TIMP-1 expression levels, aberrant glycosylation, and transcription levels of the GnT-V gene. *Closed circle* indicates an acquisition of β1,6-GlcNAc moiety on TIMP-1 molecule; *open circle* indicates a normal glycosylation of TIMP-1; diameters of *circles* indicate a relative TIMP-1 level in cancerous tissues compared with that in normal tissues. *B*, proteins were extracted from normal and cancer tissues from resection materials of colon cancer cases and precleaned with anti-mouse IgM-agarose beads. Immunoprecipitation was performed using the conjugates of an anti-TIMP-1 monoclonal antibody. The immunoprecipitates were subjected to both immunoblot and lectin blot using L-PHA. *C*, transcription levels of GnT-V were monitored by RT-PCR using two primers: 5'-tgtgtatggcaaagtggata-3' (forward) and 5'-accatggtttt-tcacgtaac-3' (backward). *D*, actin from normal and cancer tissues were compared by immunoblot analysis.

the binding affinity for active gelatinases and the inhibition ability of gelatinases (Table II). The complete structure of TIMP-1 and the inhibition mechanism was determined by X-ray crystallographic studies of the TIMP-1-MMP-3 complex (42). A wedge shaped TIMP-1 slots into the active site cleft of

an MMP in a manner similar to that of the substrate. In this study, unglycosylated TIMP-1 was crystallized to elucidate the MMP inhibition mechanism. However, several lines of evidence suggest that the glycan moiety of a glycoprotein has a decisive influence on protein-protein interactions and that a change in glycan structure of a single protein could lead to significant alterations in behavior, development, or the physiology of cells. A Fringe-catalyzed addition of a GlcNAc moiety to the fucose on Notch confers a significant strength in Notch-Delta interactions during the development of Drosophila wing (43, 44), and the hypoglycosylation of dystroglycan is related to the mitigated interaction with the substrate protein laminin, resulting in weakened cell-extracellular matrix adhesion (45). Our results (Figs. 4 and 5) and the previous report (19) taken together, the aberrant glycans on TIMP-1 may affect the properties of binding with gelatinases, presumably by conferring a steric hindrance arising from the massiveness of glycosylation and an electrostatic repulsion arising from the attachment of acidic residues to the binding to gelatinases. The structural properties for the mitigated inhibition of the aberrant TIMP-1 (TIMP-1$_{ab}$) on gelatinases await the resolution of the gelatinase-TIMP-1$_{ab}$ complex structure.

One important event necessarily accompanied in the development and progression of colon cancer is the stromal invasion and traverse of the basement membrane. This process facilitates the progression of adenomas to carcinomas and the metastasis of carcinomas. A special class of enzyme implicated in this process is MMP, which constitutes a large family, including collagenases, gelatinases, stromelysins, and membrane type-MMPs. The expression and gelatinolytic activity of MMP-9 and active MMP-2 are closely associated with cancer progression and metastasis in various types of cancer, such as cervical (46), renal (47), and ovarian (48) cancer as well as colon cancer (41). Considering the important role of gelatinases in cancer progression, the notion that an aberration of TIMP-1, a major inhibitor of gelatinases, could provide the driving force for cancer progression is likely to be pertinent.

Our knowledge of the biological behavior of MMPs and TIMPs and the roles in various diseases have an eventual goal of therapeutic uses and clinical trials of anti-cancer agents. The current trend for blocking cancer progression involves either the inhibition of MMP activity using synthetic MP inhibitors or increasing the local concentration of TIMPs by the administration of a recombinant protein or gene transfer. However, lack of efficacy and untoward side effects have made the clinical trials disappointing. Here, we suggest the relevance of the "quality control" of TIMP-1 for preventing cancer progression and malignant transformation. From this viewpoint, the development of a specific inhibitor of GnT-V and attempts to block the elongation of polylactosamine may be pertinent to such quality control. Besides, it is suggestive that, when integrated with the data of TIMP-1 expression level, the glycosyl pattern of TIMP-1 could provide important information on the

diagnostic/prognostic estimation of colon cancer.

REFERENCES

1. Parkin, D. M., Pisani, P., and Ferlay, J. (1999) Global cancer statistics. *CA.-Cancer J. Clin.* **49,** 33–64
2. Petersen, G. M., Brensinger, J. D., Johnson, K. A., and Giardiello F. M. (1999) Genetic testing and counseling for hereditary forms of colorectal cancer. *Cancer* **86,** 2540–2550
3. Powell, S. M., Petersen, G. M., Krush, A. J., Booker, S., Jen, J., Giardiello, F. M., Hamilton, S. R., Vogelstein, B., and Kinzler, K. W. (1993) Molecular diagnosis of familial adenomatous polyposis. *N. Engl. J. Med.* **329,** 1982–1987
4. Dennis, J. W., Laferte, S., Waghorne, C., Breitman, M. L., and Kerbel, R. S. (1987) Beta 1–6 branching of Asn-linked oligosaccharides is directly associated with metastasis. *Science* **236,** 582–585
5. Ihara, S., Miyoshi, E., Ko, J. H., Murata, K., Nakahara, S., Honke, K., Dickson, R. B., Lin, C. Y., and Taniguchi, N. (2002) Prometastatic effect of N-acetylglucosaminyltransferase V is due to modification and stabilization of active matriptase by adding beta 1–6 GlcNAc branching. *J. Biol. Chem.* **277,** 16960–16967
6. Guo, H.-B., Lee, I., Kamar, M., Akiyama, S. K., and Pierce, M. (2002) Aberrant N-glycosylation of β1 integrin causes reduced $\alpha 5 \beta 1$ integrin clustering and stimulates cell migration. *Cancer Res.* **62,** 6837–6845
7. Guo, H.-B., Lee, I., Kama, M., and Pierce, M. (2003) *N*-acetylglucosaminyltransferase V expression levels regulate cadherin-associated homotypic cell-cell adhesion and intracellular signaling pathways. *J. Biol. Chem.* **278,** 52412–52424
8. Mueller, M. M., and Fusenig, N. E. (2004) Friends or foes: bipolar effects of the tumour stroma in cancer. *Nat. Rev. Cancer* **4,** 839–849
9. Lewis, M. P., Lygoe, K. A., Nystrom, M. L., Anderson, W. P., Speight, P. M., Marshall, J. F., and Thomas, G. J. (2004) Tumour-derived TGF-beta1 modulates myofibroblast differentiation and promotes HGF/SF-dependent invasion of squamous carcinoma cells. *Br. J. Cancer* **90,** 822–832
10. Lohr, M., Schmidt, C., Ringel, J., Kluth, M., Muller, P., Nizze, H., and Jesnowski, R. (2001) Transforming growth factor-beta1 induces desmoplasia in an experimental model of human pancreatic carcinoma. *Cancer Res.* **61,** 550–555
11. Stetler-Stevenson, W. G., and Yu, A. E. (2001) Proteases in invasion: matrix metalloproteinases. *Semin. Cancer Biol.* **11,** 143–152
12. Kim, Y. S., Hwang, S. Y., Oh, S., Sohn, H., Kang, H. Y., Lee, J. H., Cho, E. W., Kim, J. Y., Yoo, J. S., Kim, N. S., Kim, C. H., Miyoshi, E., Taniguchi, N., and Ko, J. H. (2004) Identification of target proteins of N-acetylglucosaminyl-transferase V and fucosyltransferase 8 in human gastric tissues by glycemic approach. *Proteomics* **4,** 3353–3358
13. Kim, Y.-S., Kang, H.-Y., Kim, J.-Y., Oh, S., Kim, C.-H., Ryu, C. J., Miyoshi, E., Taniguchi, N., and Ko, J. H. (2006) Identification of target proteins of N-acetylglucosaminyltransferase V in human colon cancer and implications of protein tyrosine phosphatase kappa in enhanced cancer cell migration. *Proteomics* **6,** 1187–1191
14. Chen, T. R., Drabkowski, D., Hay, R. J., Macy, M., and Peterson, W., Jr. (1987) WiDr is a derivative of another colon adenocarcinoma cell line, *HT-29. Cancer Genet. Cytogenet.* **27,** 125–134
15. Fridman, R., Fuerst, T. R., Bird, E., Hoyhtya, M., Oelkuct, M., Kraus, S., Komarek, D., Liotta, L. A., Berman, M. L., and Stetler-Stevenson, W. G. (1992) Domain structure of human 72-kDa gelatinase/type IV collagenase: characterization of proteolytic activity and identification of the tissue inhibitor of metalloproteinase-2 (TIMP-2) binding regions. *J. Biol. Chem.* **267,** 15398–15405
16. Olson, M. W., Gervasi, D. C., Mobashery, S., and Fridman, R. (1997) Kinetic analysis of the binding of human matrix metalloproteinase-2 and -9 to tissue inhibitor of metalloproteinase (TIMP)-1 and TIMP-2. *J. Biol. Chem.* **272,** 29975–29983
17. Sagi, D., Kienz, P., Denecke, J., Marquardt, T., and Peter-Katalinic, J. (2005) Glycoproteomics of N-glycosylation by in-gel deglycosylation and matrix-assisted laser desorption/ionisation-time of flight mass spectrometry mapping: application to congenital disorders of glycosylation. *Proteomics* **5,** 2689–2701
18. Egeblad, M., and Werb, Z. (2002) New functions for the matrix metalloproteinases in cancer progression. *Nature Rev.* **2,** 161–174
19. Caterina, N. C., Windsor, L. J., Bodden, M. K., Yermovsky, A. E., Taylor, K. B., Birkedal-Hansen, H., and Engler, J. A. (1998) Glycosylation and NH2-terminal domain mutants of the tissue inhibitor of metalloproteinases-1 (TIMP-1). *Biochim. Biophys. Acta* **14,** 21–34
20. Thaysen-Andersen, M., Thogersen, I. B., Nielsen, H. J., Lademann, U., Brunner, N., Enghild, J. J., and Hojrup, P. (2007) Rapid and individual-specific glycoprofiling of a low-abundant N-glycosylated protein tissue inhibitor of metalloproteinases-1. *Mol. Cell. Proteomics* **6,** 638–647
21. Garbett, E. A., Reed, M. W., and Brown, N. J. (1999) Proteolysis in colorectal cancer. *Mol. Pathol.* **52,** 140–145
22. Ogiwara, K., Takano, N., Shinohara, M., Murakami, M., and Takahashi, T. (2005) Gelatinase A and membrane-type matrix metalloproteinases 1 and 2 are responsible for follicle rupture during ovulation in the medaka. *Proc. Natl. Acad. Sci. U. S. A.* **102,** 8442–8447
23. Stricklin, G. P. (1986) Human fibroblast tissue inhibitor of metalloproteinases: glycosylation and function. *Coll. Relat. Res.* **6,** 219–228
24. Murphy, G., Willenbrock, F., Ward, R. V., Cockett, M. I., Eaton, D., and Docherty, A. J. (1992) The C-terminal domain of 72 kDa gelatinase A is not required for catalysis, but is essential for membrane activation and modulates interactions with tissue inhibitors of metalloproteinases. *Biochem. J.* **283,** 637–641
25. Willenbrock, F., Crabbe, T., Slocombe, P. M., Sutton, C. W., Docherty, A. J., Cockett, M. I., O'Shea, M., Brocklehurst, K., Phillips, I. R., and Murphy, G. (1993) The activity of the tissue inhibitors of metalloproteinases is regulated by C-terminal domain interactions: a kinetic analysis of the inhibition of gelatinase. *Biochemistry* **32,** 4330–4337
26. O'Connell, J. P., Willenbrock, F., Docherty, A. J., Eaton, D., and Murphy, G. (1994) Analysis of the role of the COOH-terminal domain in the activation, proteolytic activity, and tissue inhibitor of metalloproteinase interactions of gelatinase B. *J. Biol. Chem.* **269,** 14967–14973
27. Heppner, K. J., Matrisian, L. M., Jensen, R. A., and Rodgers, W. H. (1996) Expression of most matrix metalloproteinase family members in breast cancer represents a tumor-induced host response. *Am. J. Pathol.* **149,** 273–282
28. Baker, E. A., Bergin, F. G., and Leaper, D. J. (2000) Matrix metalloproteinases, their tissue inhibitors and colorectal cancer staging. *Br. J. Surg.* **87,** 1215–1221
29. Yoshikawa, T., Tsuburaya, A., Kobayashi, O., Sairenji, M., Motohashi, H., Yanoma, S., and Noguchi, Y. (2001) Intratumoral concentrations of tissue inhibitor of matrix metalloproteinase 1 in patients with gastric carcinoma a new biomarker for invasion and its impact on survival. *Cancer* **91,** 1739–1744
30. Huang, L. W., Garrett, A. P., Bell, D. A., Welch, W. R., Berkowitz, R. S., and Mok, S. C. (2000) Differential expression of matrix metalloproteinase-9 and tissue inhibitor of metalloproteinase-1 protein and mRNA in epithelial ovarian tumors. *Gynecol. Oncol.* **77,** 369–376
31. Khokha, R. (1994) Suppression of the tumorigenic and metastatic abilities of murine B16F10 melanoma cells in vivo by the overexpression of the tissue inhibitor of the metalloproteinases-1. *J. Natl. Cancer Inst.* **86,** 299–304
32. Watanabe, M., Takahashi, Y., Ohta, T., Mai, M., Sasaki, T., and Seiki, M. (1996) Inhibition of metastasis in human gastric cancer cells transfected with tissue inhibitor of metalloproteinase 1 gene in nude mice. *Cancer* **77,** 1676–1680

33. Nii, M., Kayada, Y., Yoshiga, K., Takada, K., Okamoto, T., and Yanagihara, K. (2000) Suppression of metastasis by tissue inhibitor of metalloproteinase-1 in a newly established human oral squamous cell carcinoma cell line. *Int. J. Oncol.* **16,** 119–124

34. Coussens, L. M., and Werb, Z. (1996) Matrix metalloproteinases and the development of cancer. *Chem. Biol.* **3,** 895–904

35. Reed, J. C. (2001) Mechanisms of apoptosis avoidance in cancer. *Curr. Opin. Oncol.* **11,** 68–75

36. Holten-Andersen, M. N., Stephens, R. W., Nielsen, H. J., Murphy, G., Christensen, I. J., Stetler-Stevenson, W., and Brunner, N. (2000) High preoperative plasma tissue inhibitor of metalloproteinase-1 levels are associated with short survival of patients with colorectal cancer. *Clin. Cancer Res.* **6,** 4292–4299

37. Ylisirnio, S., Hoyhtya, M., and Turpeenniemi-Hujanen, T. (2000) Serum matrix metalloproteinases-2, -9 and tissue inhibitors of metalloproteinases-1, -2 in lung cancer–TIMP-1 as a prognostic marker. *Anticancer Res.* **20,** 1311–1316

38. Yoshikawa, T., Tsuburaya, A., Kobayashi, O., Sairenji, M., Motohashi, H., Yanoma, S., and Noguchi, Y. (2000) Prognostic value of tissue inhibitor of matrix metalloproteinase-1 in plasma of patients with gastric cancer. *Cancer Lett.* **151,** 81–86

39. Rhee, J.-S., Diaz, R., Korets, L., Graeme Hodgson, J., and Coussens, L. M. (2004) TIMP-1 alters susceptibility to carcinogenesis. *Cancer Res.* **64,** 952–961

40. Guedez, L., McMarlin, A. J., Kingma, D. W., Bennett, T. A., Stetler-Stevenson, M., and Stetler-Stevenson, W. G. (2001) Tissue inhibitor of metalloproteinase-1 alters the tumorigenicity of Burkitt's lymphoma via divergent effects on tumor growth and angiogenesis. *Am. J. Pathol.* **158,** 1207–1215

41. Papadopoulou, S., Scorilas, A., Arnogianaki, N., Papapanayiotou, B., Tzimogiani, A., Agnantis, N., and Talieri, M. (2001) Expression of gelatinase-A (MMP-2) in human colon cancer and normal colon mucosa. *Tumour Biol.* **22,** 383–389

42. Gomis-Ruth, F. X., Maskos, K., Betz, M., Bergner, A., Huber, R., Suzuki, K., Yoshida, N., Nagase, H., Brew, K., Bourenkov, G. P., Bartunik, H., and Bode, W. (1997) Mechanism of inhibition of the human matrix metalloproteinase stromelysin-1 by TIMP-1. *Nature* **389,** 77–81

43. Moloney, D. J., Panin, V. M., Johnston, S. H., Chen, J., Shao, L., Wilson, R., Wang, Y., Stanley, P., Irvine, K. D., Haltiwanger, R. S., and Vogt, T. F. (2000) Fringe is a glycosyltransferase that modifies Notch. *Nature* **406,** 369–375

44. Bruckner, K., Perz, L., Clausen, H., and Cohen, S. (2000) Glycosyltransferase activity of Fringe modulates Notch-Delta interactions. *Nature* **406,** 411–415

45. Michele, D. E., Barresi, R., Kanagawa, M., Saito, F., Cohn, R. D., Satz, J. S., Dollar, J., Nishino, I., Kelley, R. I., Somer, H., Straub, V., Mathews, K. D., Moore, S. A., and Campbell, K. P. (2002) Post-translational disruption of dystroglycan-ligand interactions in congenital muscular dystrophies. *Nature* **418,** 417–422

46. Fundyler, O., Khanna, M., and Smoller, B. R. (2004) Metalloproteinase-2 expression correlates with aggressiveness of cutaneous squamous cell carcinomas. *Mod. Pathol.* **17,** 496–502

47. Slaton, J. W., Inoue, K., Perrotte, P., El-Naggar, A. K., Swanson, D. A., Fidler, I. J., and Dinney, C. P. (2001) Expression levels of genes that regulate metastasis and angiogenesis correlate with advanced pathological stage of renal cell carcinoma. *Am. J. Pathol.* **158,** 735–743

48. Furuya, M., Ishikura, H., Nemori, R., Shibata, M., Fujimoto, S., and Yoshiki, T. (2001) Clarification of the active gelatinolytic sites in human ovarian neoplasms using *in situ* zymography. *Hum. Pathol.* **32,** 163–168